COBEM 2021 26th International Congress of Mechanical Engineering
ABCM Associação Brasileira de Engenharia e Ciências Mecânicas
November 22-26, 2021, Virtual Congress, Brazil

COBEM2021-0123
INFLUENCE OF CUTTING PARAMETERS IN SURFACE ROUGHNESS AND BURR FORMATION DURING HYBRID MANUFACTURING OF 316L STAINLESS STEEL

Bianca de Souza Tarasco
Gabriel Mencarini Castanheira
Raphael de Souza Costa
Vanessa Seriacopi
Adalto de Farias
Guilherme Wolf Lebrão
Instituto Mauá de Tecnologia, Praça Mauá, 01 – São Caetano do Sul/SP – 09580-900
biancatarasco97@gmail.com
gabriel.mencarini2@gmail.com
raphaelcosta95@hotmail.com
vanessa.seriacopi@maua.br
adalto.farias@maua.br
guinet@maua.br

Gilmar Ferreira Batalha
Escola Politécnica da Universidade de São Paulo - Av. Prof. Luciano Gualberto, 380 – São Paulo/SP - 05508-010
gfbatalh@usp.br

Éd Claudio Bordinassi
Instituto Mauá de Tecnologia, Praça Mauá, 01 – São Caetano do Sul/SP – 09580-900
ecb@maua.br

Abstract. *Additive manufacturing has been growing up in recent years, mainly for small parts, complex geometries, and materials as titanium alloys and stainless steels used in medicine applications. The surface roughness in additive manufacturing is high and, for some applications, another process must be used to finish the part surface, and in this case hybrid manufacturing is an alternative. The objective of this paper was to analyze the influence of laser power (used in additive manufacturing) and cutting parameters (in milling), in the surface roughness and burr formation during hybrid manufacturing. AISI 316L stainless steel parts were manufactured using the direct metal laser sintering (DMLS) technique with laser powers of 160 and 190 W. A factorial experimental design was applied and 32 parts were manufactured, varying the cutting parameters for both laser powers: feed rate, cutting speed, cutting depth, and use of fluid. Characterizations were performed to measure the average roughness, using a portable profilometer, and the height of the burr, using a profile projector. The data of the surface roughness and burr measurements were statistically analyzed in the Minitab software, generating graphs of the main effects and interactions, which made possible the evaluation of the influence of each parameter of the hybrid manufacture in the surface finishing. The cutting depth was the parameter that most influenced the average roughness of the parts, its increase generated higher roughness values. In addition, the following interactions consisted of the factors with the highest influence on the roughness of the parts, respectively: (i) the cutting depth with the laser power; (ii) the cutting depth with the presence or absence of fluid; and (iii) the cutting speed with the feed rate. In turn, the feed rate was the parameter that most affected the burr formation, and its increase raised the burr heights. The terms with the highest influence on burr formation were, respectively, the feed rate, the interaction of feed rate with cutting depth, and the interaction between all parameters, except the cutting speed. It was found that different laser power parameters in additive manufacturing influenced the surface finish.*

Keywords: *Additive Manufacturing, Hybrid Manufacturing, Burr, Surface Roughness.*

1. INTRODUCTION

The 21st century demand to innovate towards a product revolution is clearly seen and additive manufacturing, widely known as 3D printing, is a manufacturing process with direct digital technology, where a component can be produced layer by layer from the 3D model without or with minimal further use of machining, molding, or casting. It has developed rapidly over the past 10 years and has demonstrated significant potential for reducing the cost of critical performance components. This can be achieved through greater design freedom, less material waste and reduced post-processing steps

(MEGAHEAD et al, 2016). However, the quality and precision of the surface precludes its further development to produce products for users with high precision, in which Computer Numerical Control (CNC) processes on the other hand provide the ability to generate components with extremely high levels of precision and surface, but with geometry constraints (ZHU et al, 2016). Hybrid manufacturing is an interesting alternative to combine the two needs and achieve parts with significant improvements in their mechanical and surface properties.

According to ASTM 52900 standard, additive manufacturing processes (AM) are divided into 7 categories (HÄFELE et al., 2019) and one of the most used methods for manufacturing is DMLS (Direct Metal Laser Sintering), which uses powder as a raw material that is selectively melted by a concentrated laser-generated heat source, with subsequent cooling (Li et al, 2019) and layers ranging from 30 to 50 µm (BRINKSMEIER, et al., 2010).

Hybrid processes or hybrid manufacturing (use of additive manufacturing plus a second process or energy source that affects part quality, functionality or performance), (MADIREDDY et al., 2019 and HEIGEL et al., 2018) received significant attention in its ability to capitalize on the advantages of independent processes while minimizing the disadvantages (ZHU et al., 2016). A typical configuration of hybrid processes is the combination of additive and subtractive processes that integrate CNC machining and additive manufacturing processes as a new solution in the production of complex components. According to Häfele et al., (2019) a combination of additive and subtractive processes (hybrid) can guarantee a more efficient production cost, and these authors propose a systematic approach to choose the process chain according to the characteristics of the parts. The main focus of studies in recent years in AM has been heat treatment and consequent reduction of the residual stress generated during the process. Some works focused on hybrid manufacturing, such as Struzikiewicz et al., (2019) for example, who studied the turning of AISI 316L parts, comparing the cutting forces and roughness obtained as a function of the cutting parameters. Löber et al., (2013) studied different types of grinding and polishing in AISI 316L parts and analyzed the surface roughness and condition using a scanning electron microscope. The results of the work by Kaynak and Kitay (2018), who turned AISI 316L parts generated by Selective Laser Melting - SLM, showed that the roughness of the parts decreased as well as the porosity. The machining-affected layer was between 10 and 20 µm and the microhardness increased between 9 and 23%, compared to the original part. Rotella et al, (2018) also found lower roughness and higher hardness values in Ti6Al4V alloy parts made by some additive manufacturing processes and turned. Kaynak and Kitay (2019) found similar results for AISI 316L parts generated by SLM and finished by various processes.

With a focus on materials approaches, AISI 316L austenitic stainless steel is used in many industrial sectors such as marine and aerospace engineering (Yang et al., 2021), and other applications ranging from jewelry to welding. It is widely recognized for its biocompatibility, its excellent corrosion resistance, its low cost, availability and biocompatibility make it a good candidate with additive manufacturing for the manufacture of implants or orthopedic prostheses (Andreau et al., 2019). In austenitic steels, the high chromium content (up to 18%) contributes to its exceptional corrosion resistance, while the low carbon content (denoted by the letter 'L') reduces the susceptibility to forming carbides that can cause cracking by corrosion. However, 316L stainless steel and other low carbon stainless steels cannot be reinforced by heat treatment procedures, due to the inability to form reinforcing precipitates as a result of the low carbon content. Therefore, the general way to strengthen the 316 L SS alloy is through work hardening (Mohd Yusuf et al., 2021).

The objective of this work is to study the effects of manufacturing process parameters on surface roughness and burr formation during the hybrid manufacture of AISI 316L stainless steel.

2. METHODS AND MATERIALS

In this work, the material used was the AISI 316L manufactured by the SEAM - WIT | South Eastern Applied Materials Research Centre – Ireland. The EOSINT, model M280 with DLMS process was used, according to Figure 1.

Figure 1 – M280 Equipment and parts

The input parameters for AM process were: Laser speed: 1000 mm/s; Thickness: 20 µm; Laser efficiency: 100%; Laser focus: 72 µm; Laser width: 5mm; Ground Temperature: 81 °C; Laser direction rotation after each layer: 67°.

The properties for specimens after AM were: Roughness: Ra = (13 ± 5) µm; Rz = (80 ± 20) µm; Ultimate tensile strength XY direction: = (640 ± 50) MPa; Z direction = (540 ± 55) MPa; Yield stress XY direction: = (530 ± 60) MPa ; Z direction = (470 ± 90) MPa; Elastic modulus: XY direction= 185 GPa ; Z direction: = 180 GPa; Elongation XY direction = (40 ±15)%; Z direction = (50 ±20)%; Hardness: 89 HRB. The final dimensions of the parts were: 20 x 20 x 15 mm.

For the machining process, an Experimental Planning Factorial was used using the following parameters: Cutting speed (vc): 170 m/min and 210 m/min; Feed rate (fz): 0.1 mm/rot and 0.2 mm/rot; Cutting depth (ap): 0.35 and 0.7 mm; Cutting fluid: No and Yes; Laser Power: 160 and 190 W, totalizing 32 trials.

Machining was performed in a Romi Discovery 560 Center Machine , at Instituto Mauá de Tecnologia, using a face milling operation in the center of the parts, with carbide inserts: M class, code R245-12 T3 K-MM 2030; with Milling head CoroMill 245 – 45° - R245-063Q22-12M. The milling process was made at the center of the parts, being up milling in the start of the cutting and down milling at the end of cutting (face with burr formation), that means, the burr formation face was located at the exit of the cutting tool milling.

The Surftest SJ-210- Series, Portable Surface Roughness Tester was used for the surface roughness measurements.

The Mitutoyo Optical Comparator Type PJ-250V was used for the burr measurements, as illustrated in Figure 2.

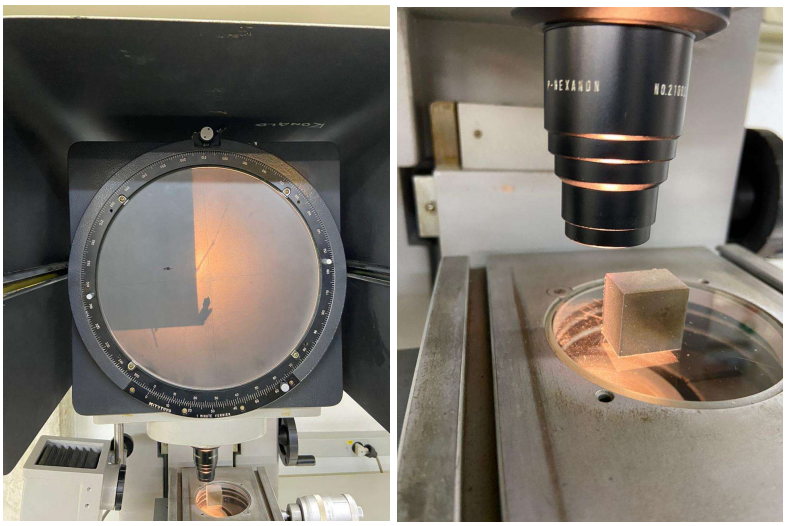

Figure 2 -Example of the burr measurement

3. RESULTS AND DISCUSSION

Table 1 shows the results of the surface roughness and burr formation measurements after the milling process.

Surface roughness ranged from 0.2 to 0.43 µm of Ra, since finishing parameters were used. The burr height ranged from 0.075 to 1.09 mm.

Figure 3 shows the Pareto Diagram for the surface roughness. The interaction between cutting depth and laser power, followed by cutting depth and the interaction between cutting depth and cutting fluid, and cutting speed and feed rate showed statistical significance in this study.

Figure 4 shows the main effects plot that corroborates the Pareto diagram. The most important variables are the cutting depth and laser power. In general, the feed rate is the most important variable when surface roughness is studied since they are geometrically dependent. In this study, higher values to cutting depth were chosen to induce most effectively results about this variable. The increase in the cutting depth causes a considerable increase in the average roughness in the part, as shown in the study by Rossi et al. (2004) which makes it clear, the cutting depth is directly proportional to the surface roughness, because the chip section to be removed from the part depends on the cutting depth, and higher cutting forces induce higher vibration, and consequently more average surface roughness.

Table 1 – Results for the roughness and burr measurements

Vc [m/min]	f [mm/rev]	ap [mm]	Fluid	Laser [W]	Ra [µm]	Burr [mm]
170	0.1	0.35	Yes	160	0.27	0.605
210	0.1	0.35	Yes	160	0.2	0.29
170	0.2	0.35	Yes	160	0.23	0.34
210	0.2	0.35	Yes	160	0.25	0.375
170	0.1	0.7	Yes	160	0.39	0.125
210	0.1	0.7	Yes	160	0.36	0.15
170	0.2	0.7	Yes	160	0.34	1.09
210	0.2	0.7	Yes	160	0.35	0.935
170	0.1	0.35	No	160	0.27	0.28
210	0.1	0.35	No	160	0.27	0.325
170	0.2	0.35	No	160	0.3	0.355
210	0.2	0.35	No	160	0.35	0.78
170	0.1	0.7	No	160	0.38	0.13
210	0.1	0.7	No	160	0.38	0.535
170	0.2	0.7	No	160	0.38	0.455
210	0.2	0.7	No	160	0.35	0.075
170	0.1	0.35	Yes	190	0.26	0.44
210	0.1	0.35	Yes	190	0.28	0.33
170	0.2	0.35	Yes	190	0.28	0.47
210	0.2	0.35	Yes	190	0.31	0.305
170	0.1	0.7	Yes	190	0.36	0.125
210	0.1	0.7	Yes	190	0.31	0.19
170	0.2	0.7	Yes	190	0.31	0.75
210	0.2	0.7	Yes	190	0.36	0.55
170	0.1	0.35	No	190	0.43	0.33
210	0.1	0.35	No	190	0.22	0.21
170	0.2	0.35	No	190	0.25	0.275
210	0.2	0.35	No	190	0.37	0.32
170	0.1	0.7	No	190	0.23	0.075
210	0.1	0.7	No	190	0.24	0.08
170	0.2	0.7	No	190	0.24	0.63
210	0.2	0.7	No	190	0.27	0.85

Higher laser power induces smaller surface roughness. These results are in agreement with Saunders (2017), who correlated the Laser Power with the porosity of the manufactured parts. Lower laser power generates more porosity. For the other three variables, smaller influences were observed, as follows: higher cutting speeds generate smaller surface roughness, increasing temperature, facilities material removal with smaller cutting forces and smaller surface roughness; higher feed rate generates higher surface roughness as expected; Dry cutting results in higher surface roughness; in this case, probably the effect of lubricant made difference in the removal of the tribological material removal and made better surfaces.

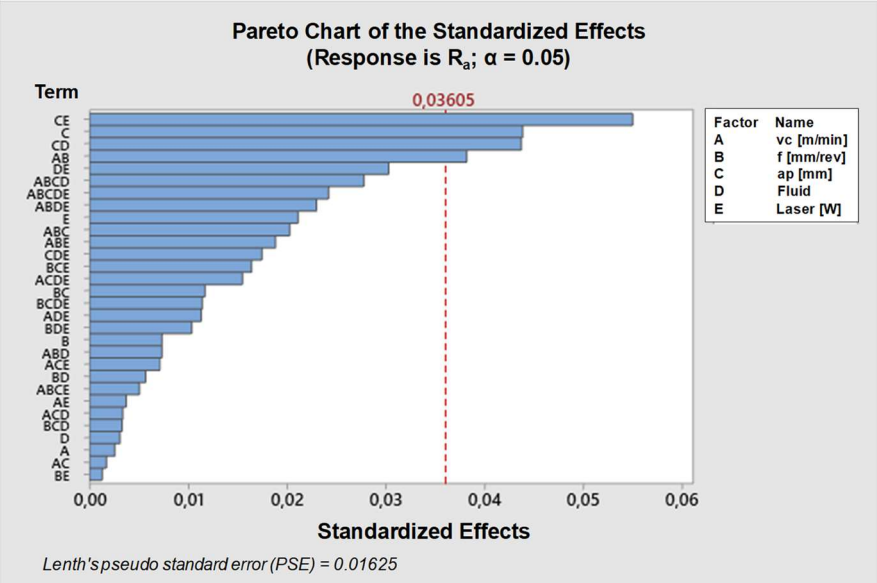

Figure 3 – Pareto Diagram for the surface roughness results

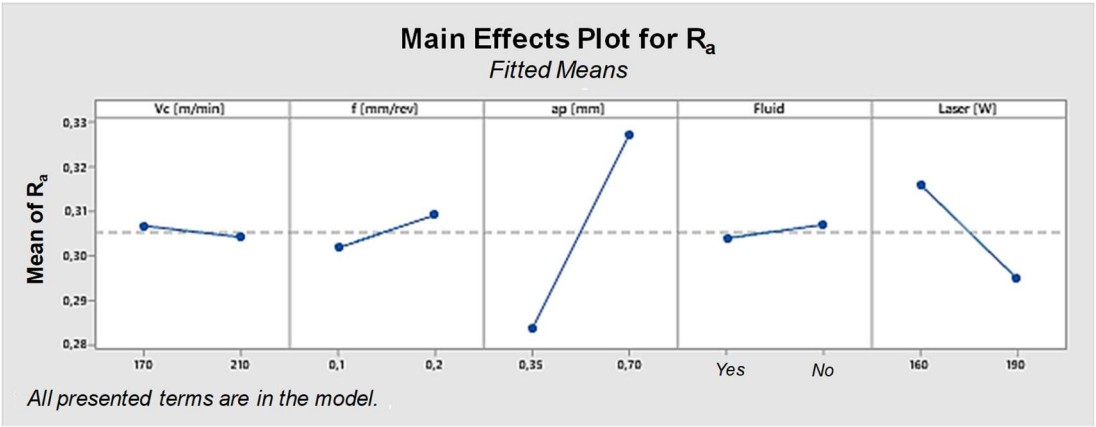

Figure 4 – Main effects plot for surface roughness results

Figure 5 shows all the contour plots for the surface roughness. The better results for the surface roughness can be noted at the last image, in the corner right below, where the lower laser power and smaller cutting depth were used. The other Figures provide a “map” to select the adequate surface roughness correlated with the input parameters.

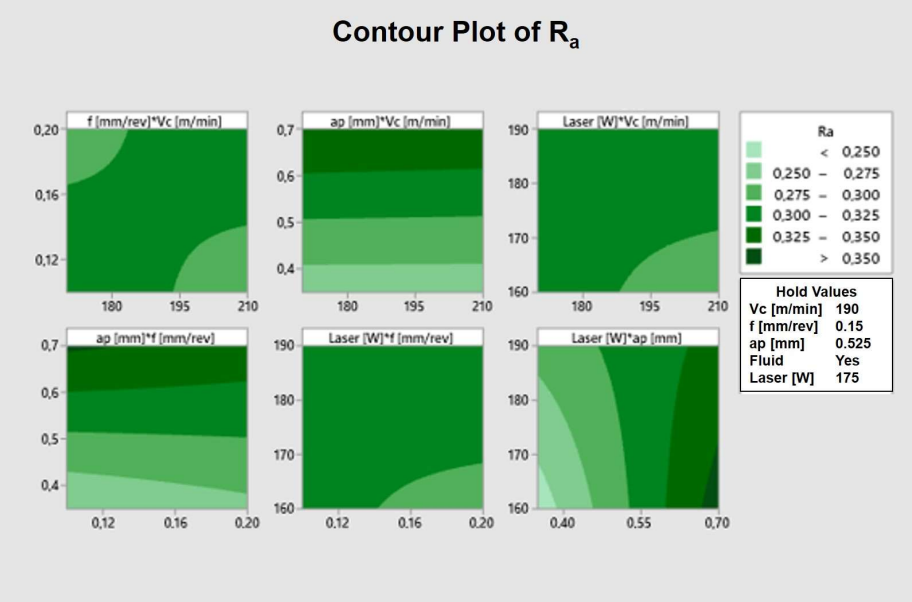

Figure 5 – Contour plots for the surface roughness results

Figure 6 shows the Pareto diagram for the burr height measurements. The feed rate followed by the interaction between the feed rate and cutting depth, and the interaction between the feed rate, cutting depth, cutting fluid, and laser power are statistically significant.

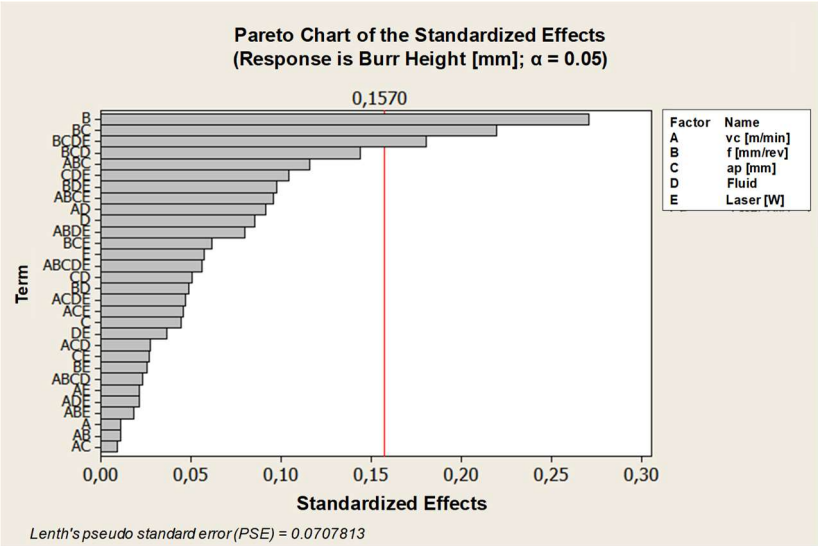

Figure 6 – Pareto Diagram for the burr height measurements

Figure 7 shows the main effects plot for the burr height measurements. The cutting speed was the input with a smaller influence on the results. The increase in the feed rate caused a significant increase in the burr height, being the parameter with the greatest individual influence, a fact observed by the slope of the straight line. According to Hajiahmadi (2019), the feed rates caused an increase in the burr height in the up-milling, because there is greater friction between the tool and the workpiece and greater efforts involved as the tool removes the material. In this case, there is no ploughing effect, which occurs when the main edge tool enters the part without shear, plastically deforming the material and pushing it down. Increasing in the cutting depth, generated a small increase in burr height, a fact that also occurred in the studies by Hajiahmadi (2019). As the cutting depth increases, the amount of material displaced by the main edge tool also increases proportionately, restricting the possibility of material flowing towards the edge, resulting in a lateral flow of material perpendicular to the edge.

The dry cutting during milling, made higher burr formation, as explained by Mendes and Silva (2003). This behavior can be explained by the drop in temperature generated with the use of the fluid, which caused an increase in the material shear strength of the parts.

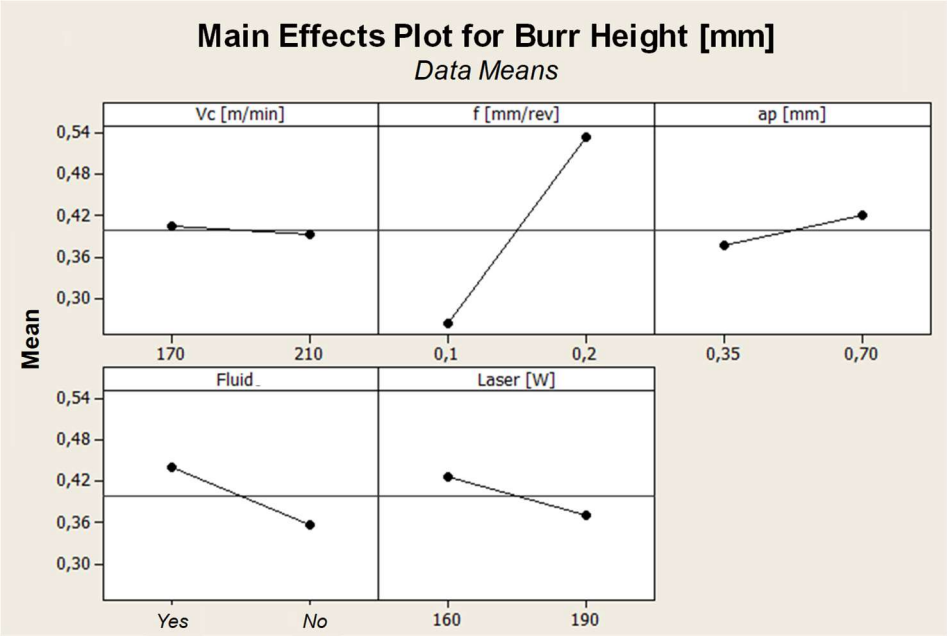

Figure 7 – Main effects plot for the burr height measurements

Increasing the laser power generated a smaller burr formation. One hypothesis for this behavior is that there was a reduction in efforts during post-processing, due to the lower porosity generated in parts produced with greater laser power, according to Sander et al (2017), thus reducing burr formation.

Figure 8 shows the main effect plot for the burr height measurements.

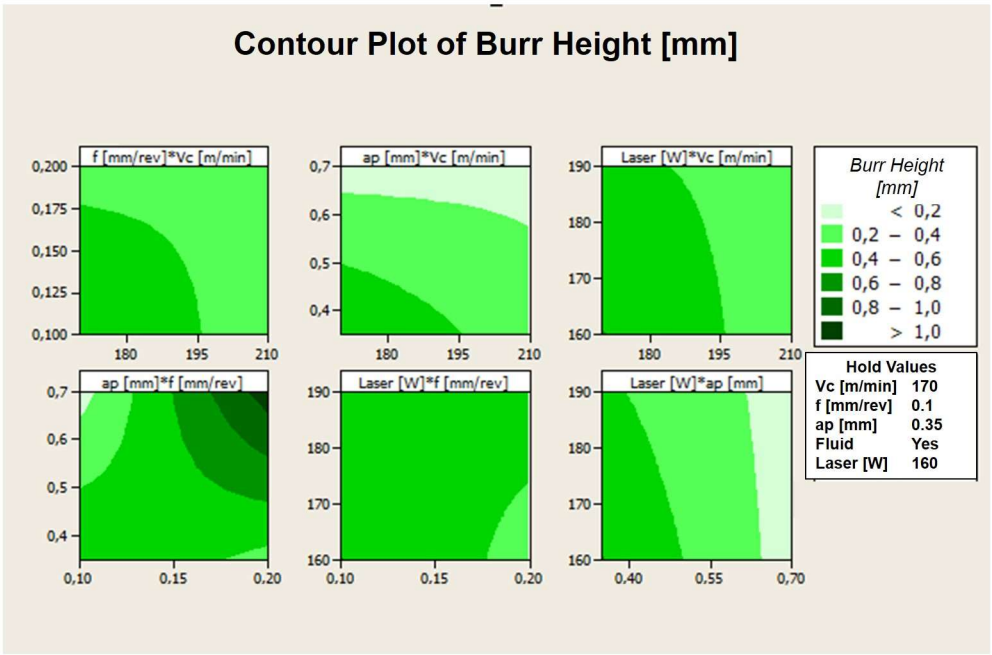

Figure 8 – Contour plot for the burr height measurements

4. CONCLUSION

The laser power influenced the generated surface, even after the milling process.
For the surface roughness, the main conclusion can be delineated as follows:

- Higher cutting depth generated higher surface roughness, and the same occurs for the higher feed rate and smaller laser power;
- With regard to cutting depth, the roughness remains constant with dry cutting but increases significantly with the increase of cutting depth in the presence of fluid;

In burr formation, the terms of greatest influence were, respectively:

- The increase in the feed rate, generated a significant increase in burr formation;
- In a small scale, the increase in the cutting depth increases the burr height. Smaller laser power and the use of cutting fluid also generated a higher burr height.

5. REFERENCES

Andreau O., Koutiri I., Peyre P., Penot J.D., Saintier N., Pessard E., De Terris T., Dupuy C., Baudin T., 2019. Texture control of 316L parts by modulation of the melt pool morphology in selective laser melting. Journal of Materials Processing Technology. 264, 21–31. https://doi.org/10.1016/j.jmatprotec.2018.08.049

Hafele T., Schneberger J., Kaspar J., Vielhaber M., Griebsch J., 2019. Hybrid addictive manufacturing - process chain correlations and impacts. Procedia CIRP, v. 84, p. 329-344.

Hajiahmadi S., 2019. Burr size investigation in micro milling of stainless steel 316L. International Journal of Lightweight Materials and Manufacture, v. 2, n. 4, p. 296–304.

Heigel J.C., Phan T.Q., Fox J.C., Gnaupel-Herold T.H., 2018. Experimental Investigation of Residual Stress and its Impact on Experimental Investigation of Residual Stress and its Impact on Machining in Hybrid Additive / Subtractive Manufacturing, Procedia Manufacturing, v. 26, p. 929-940.

Kaynak Y., Kitay O., 2019. The effect of post-processing operations on surface characteristics of 316L stainless steel produced by selective laser melting. Additive Manufacturing, v. 26, p. 84–93. https://doi.org/10.1016/j.addma.2018.12.021

Li N., Huang S., Zhang G., Qin R., Liu W., Xiong H., Blackburn J., 2019. Progress in additive manufacturing on new materials: A review. Journal of Materials Science and Technology, v. 35(2), p. 242–269. https://doi.org/10.1016/j.jmst.2018.09.002

Löber L., Flache C., Petters R., Kühn U., Eckert J., 2013. Comparison of different post processing technologies for SLM generated 316l steel parts. Rapid Prototyping Journal, v. 19(3), p. 173–179. https://doi.org/10.1108/13552541311312166

Madireddy G., Li C., Liu J., Sealy M.P., 2019. Modeling thermal and mechanical cancellation of residual stress from hybrid additive manufacturing by laser peening. Nanotechnology and Precision Engineering, v. 2, p. 49–60.

Megahed M., Mindt H., Dri N.N., Duan H., Desmaison O., 2019. Metal additive-manufacturing process and residual stress modeling. Integrating Materials and Manufacturing Innovation. https://doi.org/10.1186/s40192-016-0047-2

Mendes, A.L.S; Da Silva, M.B., 2005. Estudo da formação de rebarbas formadas em usinagem. Universidade Federal de Uberlândia.

Mohd Yusuf S., Lim D., Chen Y., Yang S., Gao N., 2021. Tribological behaviour of 316L stainless steel additively manufactured by laser powder bed fusion and processed via high-pressure torsion. J. Mater. Process. Technol. 290. https://doi.org/10.1016/j.jmatprotec.2020.116985

Process. Technol. 270, 8–19. https://doi.org/10.1016/j.jmatprotec.2019.01.028

Rotella G., Imbrogno S., Candamano S., Umbrello D., 2018. Surface integrity of machined additively manufactured Ti alloys. Journal of Materials Processing Technology, v. 259, p. 180–185. https://doi.org/10.1016/j.jmatprotec.2018.04.030

Saunders, M., 2017. X marks the spot - find ideal process parameters for your metal AM parts. Linkedin, Disponível em: https://www.linkedin.com/pulse/x-marks-spot-find-ideal-process-parameters-your-metal-marc-saunders/. Acesso em: 15 de Out. de 2020.

Struzikiewicz G., Zebala W., Matras A., Machno M., Ślusarczyk Ł., Hichert S., Laufer F., 2019. Turning research of additive laser molten stainless steel 316L obtained by 3D printing. Materials, v. 12(1), p. 1-14. https://doi.org/10.3390/ma12010182

Yang Y., Gong Y., Li C., Wen X., Sun J., 2021. Mechanical performance of 316 L stainless steel by hybrid directed energy deposition and thermal milling process. J. Mater. Process. Technol. 291. https://doi.org/10.1016/j.jmatprotec.2020.117023

Zhu Z., Dhokia V., Nassehi A., Newman S.T., 2016. Robotics and Computer-Integrated Manufacturing Investigation of part distortions as a result of hybrid manufacturing, Robotics and Computer Integrated Manufacturing, v. 37, p. 23–32. https://doi.org/10.1016/j.rcim.2015.06.001

6. RESPONSIBILITY NOTICE

The authors are the only responsible for the printed material included in this paper.